Technical University of Denmark

Full-scale Milling Tests of Wood Pellets for Combustion in a Suspension-Fired Power Plant Boiler

Masche, Marvin; Puig Arnavat, Maria; Wadenbäck, Johan ; Clausen, Sønnik; Jensen, Peter Arendt; Ahrenfeldt, Jesper; Henriksen, Ulrik Birk

Publication date:
2017

Document Version
Peer reviewed version

Full-scale Milling Tests of Wood Pellets for Combustion in a Suspension-Fired Power Plant Boiler

Marvin Masche[1*], Maria Puig-Arnavat[1], Johan Wadenbäck[2], Sønnik Clausen[1], Peter A. Jensen[1], Jesper Ahrenfeldt[1], Ulrik B. Henriksen[1]

[1]*Department of Chemical and Biochemical Engineering,*

Technical University of Denmark, 2800 Kgs. Lyngby, Denmark

[2]*Amagerværket, HOFOR A/S, Kraftværksvej 37, 2300 Copenhagen S, Denmark*

[*]*Corresponding author. E-mail address: marv@kt.dtu.dk*

Abstract – The size reduction of pelletized wood is crucial in suspension-fired power plants, and hence its milling characteristics are of interest to optimize the milling and combustion process. The objective of the study was to compare the size and shape of pellets disintegrated in hot water with that from pellets comminuted at different mill loads. The milling performance of two industrial wood pellet qualities in large-scale coal vertical roller mills at different mill operating conditions was studied. The milling performance was assessed by determining the specific grinding energy consumption (SGEC), and analyzing the comminuted particle shape and particle size distribution (PSD). Large-scale pellet comminution produced finer and wider PSDs than pellet disintegration in hot water, but only slightly altered the particle shape. The mill pressure loss, absorbed mill power, and hence SGEC depended on the pellet quality. Decreasing the mill load produced finer and wider PSDs, and reduced the mill pressure loss and absorbed mill power. However, the SGEC was negatively correlated with the mill load. Adjustments of mill operating conditions had a minor effect on the comminuted particle shape.

1. Introduction

The production and trade of industrial wood pellets as a renewable energy commodity for heat and power generation have experienced a tremendous growth over the past decade in Europe [1], [2]. European energy policies have driven this development to mitigate greenhouse gas emissions [3]. Northern European countries, such as Sweden, Denmark and United Kingdom have converted, or are currently converting their existing combined heat and power (CHP) plants from coal to operate on renewable biomass, mostly wood pellets, to meet the European '20-20-20' climate targets by 2020 [1]. One example of successful conversion from coal to biomass pellets of a suspension-fired power plant is Amagerværket unit 1 (AMV1), located in Copenhagen (Denmark). Originally designed for coal, AMV1 was converted in 2010 to operate mainly on wood pellets. For comminuting fibrous and orthotropic elastic wood that is capable of absorbing energy before size reduction [4], the existing mills were refurbished to improve the grinding efficiency by producing greater shearing forces.

The comminuted particle size and shape are important physical properties for suspension-firing, as they influence the particle dynamics, particle heat and mass transfer [5]. Thus, the energy intensive size reduction step in power plants needs to be optimized for wood pellets. Generally, comminuting lignocellulosic biomass requires more energy than coal regardless of mill type [6]. The energy required for milling biomass depends on the feed moisture, particle size reduction ratio, feed characteristics [7], feed rate and mill operating parameters [8]. To achieve complete particle combustion for coal suspension-firing, there are particle size limits for the classifier [9]. Equivalent limits for woody biomass particles have not been established. A size reduction to the same level as pulverized coal may not be required due to the high volatile content (i.e. high reactivity) of biomasses in combustion systems [10]. Esteban and Carrasco [11] recommend 95 % of wood particles (dry weight basis) to be below 1 mm for optimal combustion in a pilot-scale pulverized fuel burner. Adams et al. [12] further found that 25 % of biomass (dry weight basis) below 100 µm was ideal for excellent flame stability.

For many years, co-milling of pelletized biomasses with coal has been performed for co-firing in a number of power plants [13]. However, knowledge and experience regarding 100 % wood pellet comminution in coal mills as a crucial size reduction step for efficient combustion in a suspension-fired boiler is limited. To fill this gap in knowledge, the present paper provides a detailed full-scale grindability study of two industrial wood pellet qualities in VRMs at AMV1. To the best knowledge of the authors, no similar studies have been published in this field. The results provided can be extremely valuable to optimize the overall milling and combustion process for plant operators facing the problems of changing from coal to biomass pellets. The main objectives of the present study are:

- To compare the morphology (size and shape) of pellets disintegrated in hot water with that from pellets comminuted at different mill loads
- To compare the influence of different pellet qualities on the milling process
- To test if different mill operating conditions affect the comminuted pellet fineness

2. Materials and Methods

2.1. Materials

Two industrial wood pellet qualities (A and B pellets) were tested. A pellets were mainly softwood pellets produced in Europe (Baltic countries). B pellets were pellets made of ca. 93 % softwood and 7 % hardwood, and produced in Southeastern United States. The wood pellets were characterized in triplicate according to standardized methods (Table 1). B pellets featured a coarser internal particle size distribution (PSD). In particular, more than 79 % of the disintegrated A pellet particles were below 1 mm, while only more than 59 % of the disintegrated B pellet particles were smaller than 1 mm.

Table 1: A and B pellet characteristics.

Parameters	Unit	A Pellets	B Pellets	Method
Moisture content	wt.% as received, wet basis	6.6	5.7	EN ISO 18134-1: 2015
Ash content	wt.%, dry basis	0.6	0.6	EN ISO 18122: 2015
Volatile matter	wt.%, dry basis	84.5	83.9	EN ISO 18123: 2015
Fixed carbon	wt.%, dry basis	14.9	15.5	By difference
Carbon	wt.%, dry basis	50.7	51.1	EN ISO 16948: 2015

Nitrogen	wt.%, dry basis	0.2	0.1	EN ISO 16948: 2015
Hydrogen	wt.%, dry basis	6.1	6.1	EN ISO 16948: 2015
Oxygen	wt.%, dry basis	42.4	42.0	EN 14588:2010 (by difference)
Net calorific value	MJ/kg, as received	17.5	18.0	EN 14918: 2009
Pellet diameter (D) and length (L)	mm, as received	D, 6.2 and 8.3; L, 12.3	D, 6.7; L, 12.9	EN ISO 17829: 2015
Bulk density	kg/m3, as received	653.1	669.2	EN ISO 17828: 2015
Mechanical durability (fines)	wt.%, as received	98.5	99.1	EN ISO 17831-1: 2015
PSD of disintegrated pellets (internal PSD)	wt.%, dry basis	≥ 99.5 % (< 3.15 mm) ≥ 98.7 % (< 2.0 mm) ≥ 79.2 % (< 1.0 mm)	≥ 97.9 % (< 3.15 mm) ≥ 93.9 % (< 2.0 mm) ≥ 59.4 % (< 1.0 mm)	EN ISO 17830: 2016

2.2. Vertical roller mills and dynamic classifiers

The pellet milling process comprises comminution, drying, particle classification and product discharge to the burners. Pellets were comminuted in one of the three coal VRMs (type LM 19.2 D, Loesche GmbH, Germany) at AMV1, denoted as M20 (mill 20). In each mill, hot primary air lifts the comminuted wood particles into the spinning rotor of the dynamic classifier (or rotor classifier). Here, drag or centripetal forces (generated by the airflow to the rotor), and mass or centrifugal forces (generated by the rotor rotation) act upon the particles [14]. If the mass force is greater than the drag force, particles are rejected to the milling table for further size reduction. Else, if the drag force is greater than the mass force, the primary airflow lifts the particles through the rotor into the burner pipes [15]. The balance between both forces governs the particle separation [9]. If both forces are in equilibrium for a specific particle mass, the rotor classifies the particle with 50 % efficiency. This is referred to as the classifier cut size. Generally, the plant operator can control the classifier cut size, and thus the comminuted product fineness by adjusting the classifier rotor speed, dam ring height, milling table speed, $\dot{m}_{Air}$, HGP of the roller, and fresh $\dot{m}_{Pellet}$ [14], [16], [17]. The rollers also achieve a sliding movement that result in additional shearing forces to comminute the pellets.

2.3. Sampling equipment

Wood pellets were sampled from the end of the continuously moving conveyor belt before entering the mill. This sampling method is suggested in ISO 14488:2007 [18]. Sampling powdered material from a moving stream inside a vertical or horizontal fuel pipe is problematic. The sampling ports for dust leaving M20 are placed in vertical sections of the pipes and easy to access. Furthermore, M20 is the only mill with symmetrical pipes to the burners. Thus, to ensure minimum disturbance of the condition and composition of the flow inside the pipe, dust samples were obtained only from M20 using an isokinetic (i.e. sampling velocity = flow velocity) sampling unit with cyclone. The sampling unit inlet was calibrated to be isokinetic with a velocity of 30 m/s, which was the mean flow velocity inside the fuel pipes. The sampling unit with cyclone consisted of a pipe with one end bent 90° that was isoaxially (i.e. aligned with the flow) inserted into the fuel pipe. By vortex separation, the cyclone removed the very fine dust sucked into a filter through an outlet. Isoaxial and isokinetic sampling conditions are according to ISO 14488:2007 [20]. For shape and size analysis, dust samples were split into representative subsamples by a rotating sample divider (type PT100, Retsch Technology GmbH, Germany).

2.5. Dynamic image analysis

A dynamic image analyzer (type Camsizer® X2, Retsch Technology GmbH, Germany) recorded simultaneously the size and shape of comminuted pellets using two linked cameras (basic and zoom camera) with a resolution of 4.2 megapixel per image, covering a measuring range from 30 µm to 8 mm. The particles are individually detected as projected areas, digitalized and the images processed. The X-Jet mode of the Camsizer® X2 was used to disperse the agglomerated wood dust falling from a vibrating feeder by a compressed air-driven venturi nozzle. Preliminary tests were run to estimate the optimal compressed air pressure (30 kPa) and sample size (15-20 g). The measurements were done in triplicate.

Compared to sieving, the PSD from Camsizer® X2 is presented as a cumulative (undersize) volume distribution versus $x_{c,min.}$ Preliminary tests and previous studies [6] show that this parameter gives the closest results to those obtained by sieve analysis. Camsizer® X2 software also provides the aspect ratio (width to length ratio) and circularity values among other 2D shape parameters. These two parameters are commonly used for describing comminuted wood particle shapes [6], [19]. The aspect ratio (AR) ranging between zero and one is defined as Eq.1 as follows:

$$AR = \frac{x_{c,min}}{Fe_{max}} \tag{1}$$

Trubestkaya et al. [19] showed that Fe_{max} is suitable to represent the length of particle. The circularity indicates how closely the particle resembles a circle. A value of one corresponds to a perfect circle. The circularity is defined as follows (Eq.2):

$$Circularity = \frac{4 \cdot \pi \cdot A_{particle}}{P_{particle}^2} \tag{2}$$

2.5. Data analysis

The Rosin-Rammler-Bennet-Sperling (RRBS) model was used to describe the comminuted product PSD. It is a two-parameter distribution function expressed as a cumulative percent (undersize) distribution. Previous studies [20]–[22] showed good correlation between RRBS fitted parameters and measured milled particle sizes. The RRBS equation Eq. 3 is [23]:

$$R(d) = 100 - 100 \cdot e^{-\left(\frac{d}{d^*}\right)^n} \quad (3)$$

A plot of ln[ln[100/(100-R(d)]] against ln(d) on double logarithmic scale gives a straight line of slope n. The smaller the n-value, the wider the product PSD, whereas higher n-values imply a more uniform product distribution [24].

The 90th percentile (D90) of the cumulative (undersize) weight distribution is calculated to assess the classifier performance in terms of particle fineness of the collected wood dust. Yu et al. [25] found a very strong positive correlation between classifier cut size and product fineness (D90), as well as between cut size and fine product yield. The latter one is the ratio of mass flow rate of fine product and mass flow rate of material feed. In particular, a smaller cut size led to a finer dust collected, and smaller fine product yield.

The specific grinding energy consumption (SGEC) is a common measure to characterize the milling performance, expressed in the following Eq. 4:

$$SGEC = \frac{P}{\dot{m}_{Pellets}} \quad (4)$$

Another measure of the mill performance is the differential pressure drop (Δp) across the mill. A low drop in pressure is desirable, but factors such as $\dot{m}_{\mathrm{Pellets}}$, airflow rate ($\dot{m}_{\mathrm{Air}}$), and mill geometry lead to an increased Δp [26].

2.6. Milling tests

Table 2 shows the operating conditions for different milling scenarios at steady-state operation. The focus was on M20, as its outlet pipes were easy to access and symmetrical, thus minimizing the influence of pipe geometry on the dust flow characteristics. In total, the following 12 milling scenarios were chosen:

- Scenario 1-2: compare the size and shape of disintegrated A and B pellets versus A and B pellets comminuted at similar steady-state milling conditions, and
- Scenarios 3-8: test influences of mill load changes when milling A and B pellets.

Table 2: Mill operating conditions for various test scenarios.[1]

#	Pellets	$\dot{m}_{\mathrm{Pellet}}$ (t/h)	$\dot{m}_{\mathrm{Air}}$ (t/h)	Mill air/fuel ratio[2]	Rotor speed[3] (%)	HGP (MPa)
1	A	20.6	46.8	2.3	17.4	6.6
2	B	20.6	46.7	2.3	17.5	6.7
3	B	20.6	52.2	2.5	13.0	6.7
4	B	16.6	43.7	2.6	13.0	6.3
5	B	14.3	41.2	2.9	13.0	6.1
6	A	20.4	46.5	2.3	17.6	6.7

7	A	17.4	43.0	2.5	16.6	6.4
8	A	14.4	39.6	2.7	15.7	6.1

[1] Dam ring height and milling table speed are constant.

[2] Mill air/fuel ratio is the ratio of primary airflow rate to pellet feed rate into the VRM.

[3] Rotor speed is given as the percentage of the maximum speed.

3. Results and Discussion

3.1. Comparison between disintegrated and comminuted pellets

Table 3 shows that the d* and D90 values decrease after roller milling by 40 % and 19 % for A pellets, respectively, and by 49 % and 24 % for B pellets, respectively. This confirms the hypothesis that roller mills achieve an effective size reduction, and not only disintegrate pellets into their constituent particles after disintegration in hot water according to EN ISO 17830:2016. It is clear that comminuted particles are smaller than disintegrated ones. Due to the coarser initial feed PSD of B pellets, the calculated SRR is larger for B pellets than for A pellets. Comminuting A and B pellets seems to generate a similar PSD width (same RRBS *n*-value), but wider PSDs (lower RRBS *n*-values) than disintegrated pellets. Disintegrated pellets were thus more uniformly distributed than comminuted pellets.

Comminuted A pellets are finer than B pellets, especially in the medium to coarse size fraction (0.75 mm $\leq x_{c\_min} \leq$ 1.50 mm). Differences in the particle size may be explained by differences in the wood pellet characteristics, such as internal pellet PSD, and wood properties. In particular, the different anatomical structure and chemical composition of softwood and hardwood species may cause a different grinding behavior in the mill.

Table 3: Milling performance of comminuted A and B pellets compared to disintegrated pellets One standard deviation between pipes in parentheses.

	n	d* (mm)	D90 (mm)	SRR[1]	P (kW)	SGEC[2] (kWh/t)	Δp (kPa)
Comminuted pellet A (Scenario 1)	0.97 (0.03)	0.50 (0.10)	1.22 (0.07)	1.7	197.5 (3.1)	9.6	3.4 (0.2)
Disintegrated pellet A	1.37 (0.06)	0.83 (0.01)	1.51 (0.01)				
Comminuted pellet B (Scenario 2)	0.97 (0.08)	0.56 (0.13)	1.39 (0.07)	1.9	287.3 (3.3)	13.9	4.4 (0.1)
Disintegrated pellet B	1.40 (0.01)	1.09 (0.04)	1.82 (0.02)				

[1]SRR = size reduction ratio representing the ratio of d* of the disintegrated pellet feed to d* of the comminuted pellet product.

[2]Dynamic classifier and fan power not included in SGEC.

B pellets further required a 45 % higher power consumption, 45 % higher SGEC, and led to a 29 % higher Δp compared to milling A pellets (Table 3). The higher Δp may result from a higher accumulation of pellet material on the milling bed due to a larger quantity of coarse particles rejected by the classifier. The higher power consumption for B pellets may be mainly due to its coarser internal pellet PSD (feed particle size) before milling. Parameters such as pellet moisture content and durability that are known to affect the energy required for milling may be negligible, as they are similar for A and B pellets (Table 1).

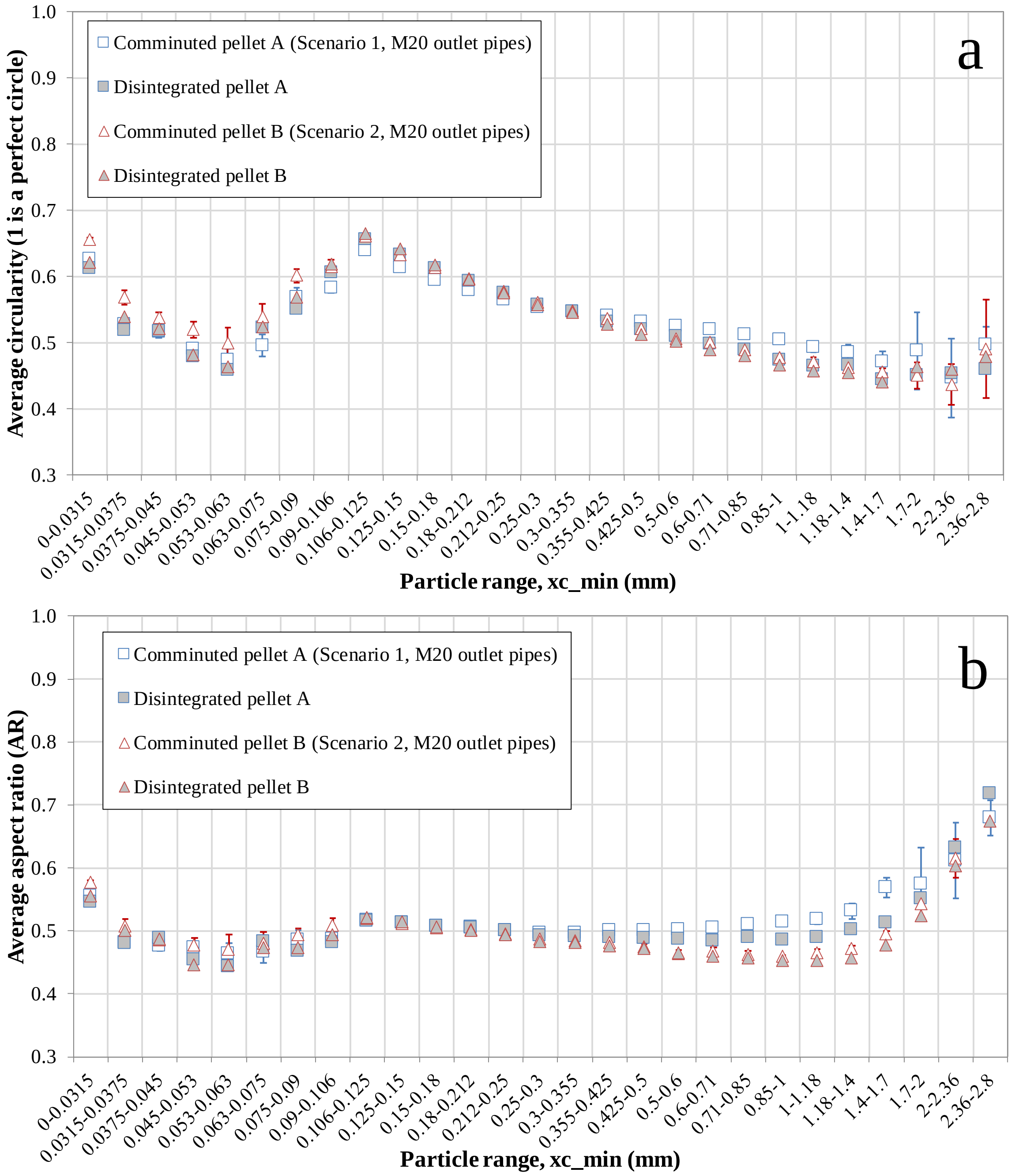

Figure 1: Average circularity (a) and aspect ratio (b) of disintegrated and comminuted A and B pellets. Error bars indicate one standard deviation within different burner pipes.

Figure 1 shows derived 2D shape parameters (aspect ratio and circularity) of comminuted and disintegrated pellet samples. Values for the coarsest particles should be taken with caution due to small number of particles analyzed. Overall, circularity and aspect ratio distributions of disintegrated and comminuted pellets show similar trends regardless the differences in internal pellet PSD. This indicates that the roller mill only affects the particle shape slightly. The observed particle shape may be therefore related to the raw material size reduction step prior to pelletization that is commonly performed in hammer mills. Pichler et al. [21] obtained similar aspect ratios for dry spruce sawdust particles ground in a hammer mill. Our experimental results also corroborate previous findings from Trubetskaya et al. [19] and Williams et al. [6] who found that comminuting pellets in roller mills only had little effect on the particle shape.

3.3. Influence of mill load

The general concept in modern CHP plants is to adjust the mill load (i.e. mill productivity) according to the needs of the boiler. A measure of the mill load is the pellet feed rate to the mill. Generally, more pellets entering the mill will increase the mill load, and hence the production rate. A higher $\dot{m}_{Pellet}$ means more material on the milling table, thus increasing the milling bed thickness that will lead to a higher Δp (Table 4). This expectation is supported by a very strong positive, but not statistically significant, trend between $\dot{m}_{Pellet}$ and Δp (r=0.80, p=0.058), as shown in Table 5. In order to compensate for a thicker milling bed that requires a higher grinding effort, $\dot{m}_{Pellet}$ was regulated along with HGP. Thus, the HGP provided by the spring-loaded roller system increases with a higher $\dot{m}_{Pellet}$ (i.e. thicker milling bed) and vice versa (Table 2). The Pearson's correlation coefficient of r=1.00 (p<0.001) confirms that there is a perfect linear relationship between $\dot{m}_{Feed}$ and HGP (Table 5). Besides increasing HGP, $\dot{m}_{Air}$ was also regulated in a strong linear manner with the $\dot{m}_{Pellet}$ (r=0.99, p<0.05). The greater amount of comminuted material in the mill requires a greater airflow volume for its transport through the classifier separation zone.

Table 4: Effect of pellet feed rate on milling performance. One standard deviation between pipes is indicated in parentheses.

	$\dot{m}_{Pellet}$ (t/h)	$\dot{m}_{air}$ (t/h)	n	d* (mm)	D90 (mm)	SRR[2]	P (kW)	SGEC[1] (kWh/t)	Δp (kPa)
Disintegrated pellet A			1.37 (0.06)	0.83 (0.01)	1.51 (0.01)				
Comminuted pellet A (Scenario 6)	20.4	46.5	0.96 (0.04)	0.57 (0.07)	1.34 (0.04)	1.5	213.6 (1.9)	10.5	2.9
Comminuted pellet A (Scenario 7)	17.4	43.0	0.93 (0.01)	0.53 (0.03)	1.29 (0.08)	1.6	204.2 (1.5)	11.7	2.4
Comminuted pellet A (Scenario 8)	14.4	39.6	0.87 (0.04)	0.41 (0.03)	1.14 (0.11)	2.0	190.7 (3.1)	13.3	2.0

Disintegrated pellet B			1.40 (0.01)	1.09 (0.04)	1.82 (0.02)				
Comminuted pellet B (Scenario 3)	20.6	52.2	1.00 (0.11)	0.77 (0.07)	1.62 (0.07)	1.4	228.9 (1.1)	11.1	3.8
Comminuted pellet B (Scenario 4)	16.6	43.7	0.95 (0.06)	0.68 (0.08)	1.53 (0.07)	1.6	192.4 (1.1)	11.6	2.8
Comminuted pellet B (Scenario 5)	14.3	41.2	0.88 (0.07)	0.46 (0.08)	1.20 (0.09)	2.4	178.5 (1.2)	12.5	2.6

[1]Dynamic classifier and fan power not included in SGEC.

[2]SRR = size reduction ratio representing the ratio of d* of the disintegrated pellet feed to d* of the comminuted pellet product.

Table 4 shows the influence of various mill loads on the milling performance of A and B pellets. The general trend shows that a lower power consumption was achieved for a lower $\dot{m}_{\mathrm{Pellet}}$. The power required for comminuting A and B pellets decreased from 213.6 kW at 20.4 t/h to 190.7 kW at 14.4 t/h for A pellets and from 228.9 kW at 20.6 t/h to 178.5 kW at 14.3 t/h for B pellets, respectively. This is because the resistance of the vertical roller moving through the milling bed decreases, as the milling bed thickness reduces. Thus, it is easier for the motor to move the rollers. The correlation matrix in Table 5 further confirms that there is a statistically significant positive relationship between absorbed mill power (P) and $\dot{m}_{\mathrm{Pellet}}$ ($r=0.88$, $p<0.05$).

Being the most power-consuming unit of the CHP plant, the SGEC is a suitable indicator of the grinding efficiency. When operating at higher loads, the roller mills achieve a lower SGEC (Table 4), hence indicating a higher grinding efficiency. A statistically significant negative correlation ($r=-0.94$, $p<0.01$) was found between SGEC and $\dot{m}_{\mathrm{Pellet}}$ (Table 5). Thus, in order to reduce the SGEC, $\dot{m}_{\mathrm{Pellet}}$ (i.e. production rate) should be maximized.

Table 4 shows the changes in the PSD of comminuted A and B pellets as a function of $\dot{m}_{\mathrm{Pellet}}$ and $\dot{m}_{\mathrm{Air}}$, and compared to disintegrated pellets. The SRR decreases with a higher mill load and it seems that the dust PSDs produced at higher loads has higher d* and D90 values that indicate a reduced residence time (lower circulation load) of the pellet material in the mill. Thus, wood particles experience fewer roller-grinding actions, which lead to a coarser comminuted product. This may be due to the increasing airflow that provides a higher air speed to sweep away coarser particles to the classifier. Hence, the classifier cut size increases with increasing mill load. Consequently, at lower mill loads, the classifier cut size decreases, and the comminuted product becomes finer.

Generally, at all loads, a wider wood dust PSD (lower RRBS *n*-value) was observed compared to disintegrated pellets. The dust PSD became wider (lower RRBS *n*-value) with a decreasing mill load. The lower the RRBS *n*-value, the finer the comminuted product. At high HGP, particles theoretically experience more destructive breakage with the development of a finer product that is lifted through the classifier out to the burner pipes [16]. However, this could not be observed in this study. Instead, the increase in the $\dot{m}_{Air}$ may be a more dominant factor to affect the classifier cut size, thus resulting in a coarser final product originating from a decreased classifier separation. In summary, the roller mills achieve lower SGEC when operating at higher loads, but the wood dust produced is coarser than at lower loads. Although the mill load was reduced by 30 %, differences of average aspect ratio and circularity values between disintegrated and comminuted pellets were minimal. They followed a similar trend as described in section 3.1. Thus, VRMs regardless of their load only slightly alter the wood particle shape.

Table 5: Pearson's correlation coefficient (r) matrix for comminuting

	$\dot{m}_{Pellet}$	$\dot{m}_{Air}$	HGP	n	d*	D90	P	SGEC	Δp
$\dot{m}_{Pellet}$	1.00								
$\dot{m}_{Air}$	0.99*	1.00							
HGP	1.00***	0.89*	1.00						
n	0.79	0.59	0.81*	1.00					
d*	0.78	0.44	0.79	0.81	1.00				
D90	0.74	0.40	0.76	0.80	1.00***	1.00			
P	0.88*	0.76	0.89*	0.62	0.71	0.66	1.00		
SGEC	-0.94**	-0.87*	-0.93**	-0.65	-0.70	-0.67	-0.73	1.00	
Δp	0.80	0.49	0.81	0.85*	0.89*	0.87*	0.74	-0.71	1.00

*p < 0.05, **p < 0.01 and ***p < 0.001.

4. Conclusion

Power plant vertical roller mills achieved an effective particle size reduction, but only slightly altered the particle shape. Wood pellet comminution at various mill loads produced finer and wider PSDs than the internal pellet PSD. Pellets with a coarser internal PSD required more energy for grinding (and hence higher SGEC), and led to a higher mill pressure loss and a coarser comminuted product. Decreasing the mill load produced finer and wider comminuted pellet PSDs, and reduced mill pressure loss and absorbed mill power, but decreased the SGEC. Adjustments of mill operating conditions had a minor effect on the particle shape.

Acknowledgements

The authors thank Energinet.dk for the financial support received as part of the ForskEL project "AUWP – Advanced Utilization of Wood Pellets" (Project number: 12325). The authors wish to thank all those involved for their considerable support and contribution to the study.

References

[1] M. Cocchi, L. Nikolaisen, M. Junginger, C. S. Goh, R. Hess, J. Jacobson, L. P. Ovard, D. Thrän, C. Hennig, M. Deutmeyer, and P. P. Schouwenberg, "Global wood pellet industry market and trade study," *IEA Bioenergy Task*, p. 190pp, 2011.

[2] S. Döring, *Power from Pellets*, vol. 1. 2015.

[3] G. Eskeland, N. Rive, and T. Mideksa, "The 2020 European climate goals and the electricity sector," *11th Annual Conference on Global Economic Analysis, Helsinki, Finland*, 2008.

[4] A. Malmgren, "Talking about the revolution," *World Coal*, 2015.

[5] C. Yin, "Biomass co-firing," *Biomass Combustion Science, Technology and Engineering*, pp. 84–105, 2013.

[6] O. Williams, G. Newbolt, C. Eastwick, S. Kingman, D. Giddings, S. Lormor, and E. Lester, "Influence of mill type on densified biomass comminution," *Applied Energy*, vol. 182, pp. 219–231, 2016.

[7] M. Temmerman, P. D. Jensen, and J. Hébert, "Von Rittinger theory adapted to wood chip and pellet milling, in a laboratory scale hammermill," *Biomass and Bioenergy*, vol. 56, pp. 70–81, 2013.

[8] S. Mani, L. G. Tabil, and S. Sokhansanj, "Grinding performance and physical properties of wheat and barley straws, corn stover and switchgrass," *Biomass and Bioenergy*, vol. 27, pp. 339–352, 2004.

[9] J. L. Afolabi, "The performance of a static coal classifier and its controlling parameters Thesis submitted to the University of Leicester for the degree of Doctor of Philosophy By Jamiu Lanre Afolabi January 2012," no. January, 2012.

[10] M. A. Saeed, G. E. Andrews, H. N. Phylaktou, and B. M. Gibbs, "Global kinetics of the rate of volatile release from biomasses in comparison to coal," *Fuel*, vol. 181, pp. 347–357, Oct. 2016.

[11] L. S. Esteban and J. E. Carrasco, "Evaluation of different strategies for pulverization of forest biomasses," vol. 166, pp. 139–151, 2006.

[12] T. N. Adams, D. R. Raymond, and C. Schmid, "Optimization of a swirl burner for pulverized- wood fuels," 1988.

[13] A. Goetzl, "Developments in the Global Trade of Wood Pellets," *Office of Industries, U.S. International Trade Commission, Washington DC, USA*, 2015.

[14] G. G. Mejeoumov, "Improved cement quality and grinding efficiency by means of closed mill circuit modeling (PhD Thesis), Texas A&M University, USA," 2007.

[15] S. Palaniandy, N. A. Kadir, and M. Jaafar, "Value adding limestone to filler grade through an ultra-fine grinding process in jet mill for use in plastic industries," *Minerals Engineering*, vol. 22, no. 7–8, pp. 695–703, 2009.

[16] T. Fahrland and K. H. Zysk, "Cements ground in the vertical roller mill fulfil the quality requirements of the market," *Cement International*, vol. 11, no. 2, pp. 64–69, 2013.

[17] D. Altun, H. Benzer, N. Aydogan, and C. Gerold, "Operational parameters affecting the vertical roller mill performance," *Minerals Engineering*, vol. 103–104, pp. 67–71, 2017.

[18] ISO, "ISO 14488: Particulate materials — Sampling and sample splitting for the

determination of particulate properties," *International Organization for Standardization, Geneva, Switzerland*, 2007.

[19] A. Trubetskaya, Y. Poyraz, R. Weber, and J. Wadenbäck, "Secondary comminution of wood pellets in power plant and laboratory-scale mills," *Fuel Processing Technology*, vol. 160, pp. 216–227, 2017.

[20] W. Pichler, A. Weidenhiller, J. Denzler, R. Goetzl, M. Pain, M. Weigl, and A. Haider, "Approaches to describe the particle properties of wood pellet feedstock," *World Bioenergy 2014, Jönköping, Sweden*, 2014.

[21] W. Pichler, A. Weidenhiller, J. Denzler, R. Goetzl, M. Pain, M. Weigl, and A. Haider, "Modelling the particle size distribution of the feedstock for pellets production," *22nd European Biomass Conference and Exhibition, Hamburg, Germany*, 2014.

[22] M. Gil and I. Arauzo, "Hammer mill operating and biomass physical conditions effects on particle size distribution of solid pulverized biofuels," *Fuel Processing Technology*, vol. 127, pp. 80–87, 2014.

[23] T. Allen, *Powder sampling and particle size determination*. Elsevier Science, 2003.

[24] G. V. Barbose-Cànovas, E. Ortega-Rivas, P. Juliano, and H. Yan, *Food powders: physical properties, processing, and functionality*, no. 1. Springer, 2005.

[25] Y. Yu, R. R. Liu, and J. Liu, "Correspondence analysis and establishment of evaluation model of classification performance indices for a turbo air classifier," *Materialwissenschaft und Werkstofftechnik*, vol. 45, no. 10, pp. 900–911, Oct. 2014.

[26] D. Lindsley, *Power Plant Control and Instrumentation: the control of boilers and HRSG systems*. Michael Faraday House, Stevenage, UK: The Institution of Engineering and Technology, 2000.

Notation

$\dot{m}_{Pellets}$	Pellet feed rate [t/h]	n	Material uniformity constant (distribution parameter) [-]
$A_{Particle}$	Particle projection area [mm^2]	P	Absorbed mill power [kW]
AR	Aspect ratio [-]	$P_{Particle}$	Particle perimeter[mm]
d	Particle size [mm]	R	Cumulative percent (undersize) distribution of a material finer than the particle size d [%]
d*	Characteristic particle size defined as the size at which 63,21 % of the PSD lies below [mm]	SGEC	Specific grinding energy consumption [kWh/t]
Fe_{max}	Maximum Feret diameter or maximum caliper diameter (= particle length) [mm]	$x_{c,min}$	Shortest maximum chord (= width of a particle projection) [mm]